Proton transfer drives protein radical formation in *Helicobacter pylori* catalase but not in *Penicillium vitale* catalase

M. Alfonso-Prieto[1,2], H. Oberhofer[3], M. L. Klein[2], C. Rovira[1,4,5*], J. Blumberger[6,*]

1. Computer Simulation & Modeling, Parc Científic de Barcelona, Baldiri Reixac 4 ,08028 Barcelona, Spain.
2. Institute for Computational Molecular Science, Temple University. 1901 N. 13th Street, Philadelphia, PA 19122, USA.
3. Department of Chemistry, University of Cambridge, Lensfield Road, Cambridge CB2 1EW, UK
4. Institut de Química Teòrica i Computacional (IQTCUB). 5. Institució Catalana de Recerca i Estudis Avançats (ICREA).
6. Department of Physics and Astronomy, University College London, London WC1E 6BT, UK.

[*]to whom correspondence should be sent: **crovira@pcb.ub.es**, **j.blumberger@ucl.ac.uk**

Supporting Information

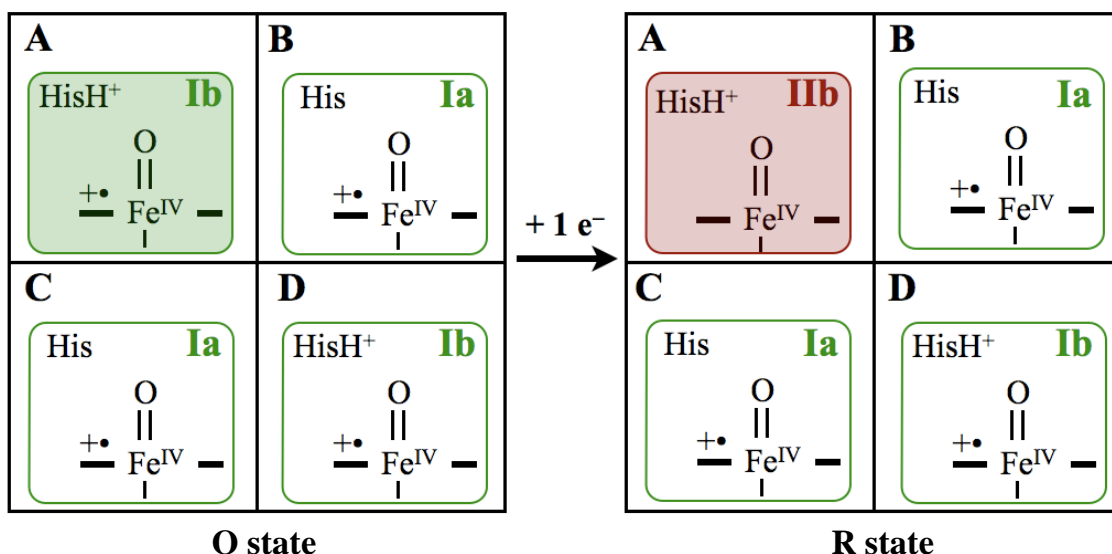# 1. Setup of the classical molecular dynamics simulations

Figure S1. Schematic representation of the oxidation and protonation states of the active site in each of the four catalase subunits (A-D), as employed in the classical molecular dynamics of the O and R states of HPC and PVC (see section 3.1 of the main text). The oxidation state of the heme is denoted as "I" and "II" (Cpd I or Cpd II, respectively). The protonation state of the distal His is indicated as "a" and "b" (neutral or protonated His, respectively).

2. Convergence of the QM/MM energy gap

2.1. Size of the QM region

The convergence of the electron affinity (ΔE, Eq. (14) in the main text) was investigated for HPC Cpd I with respect to the size of the QM region using the 10 QM/MM models shown in Figure S2. All the models correspond to the same structure, obtained from a snapshot of the oxidized state of HPC. The only difference is the size of the QM region. Model 1 includes the proximal Tyr (Tyr335, modeled as a phenolate) and the oxoferryl porphyrin with all the substituents replaced by dummy hydrogen atoms. The heme substituents are added in model 2: the methyl and vinyl groups and the propionate sidechains, which are saturated with dummy hydrogen atoms at C_α to -CH_3. Model 3 incorporates the proximal Arg (Arg339, as methylguanidinium) hydrogen-bonded to the phenolate ligand, whereas models 4 and 5 incorporate the distal histidine (His56, as methylimidazolium) and the pocket water. In models 6, 7 and 8 the other distal residues

are included too: the serine (Ser95, as methanol) hydrogen-bonded to His and one water molecule connecting it to one of the propionates of the heme, the asparagine (Asn129, as acetamide) and another water molecule hydrogen-bonded to it. In model 9 both propionate sidechains are fully included in the QM region (i.e. $-CH_2-COO^-$). Finally, in model 10 all the residues hydrogen-bonded to the propionates are included.

The electron affinities obtained for all ten QM/MM models are summarized in Table S1. The smallest QM model is clearly insufficient. The value of ΔE converges for models 4-6 at 5.17 eV before it drops by about 0.3 eV in models 7, 9 and 10. The deviation between the model used for calculation of the reduction free energy Eq. (13) (model 5), and the largest model 10 is 0.27 eV.

The different electron affinity between model 5 and model 10 can be explained by the different spin density distributions in the two models (shown in Figure S2): in model 5 the radical is delocalized over the porphyrin (i.e. the electronic configuration is Porph$^{\bullet+}$-Fe^{IV}=O), whereas in model 10 it is mainly concentrated on the oxoferryl moiety (i.e. Porph-Fe^{V}=O). Thus, the difference in electron affinity is due to insertion of the electron in a different orbital (a porphyrin-based orbital in model 5 and an iron-based orbital in model 10) to yield the reduced Cpd I (i.e. Porph-Fe^{IV}=O). This suggests that the orbital ordering is sensitive to the treatment of the electrostatic interactions between the cofactors and its surroundings, in line with previous studies on gas phase models showing that electric fields can change the orbital ordering of catalase Cpd I.[1] In the case under investigation, the classical point charge model of the propionate side chains of the heme cofactor and the hydrogen-bonded protein residues gives a good description of the electrostatics, as the spin density distribution predicted by models 1-9 is in agreement with EPR mesurements that have shown that "canonical" Cpd I bears an oxoferryl porphyrin cation radical.[2-3] Model 5 represents a good compromise between size and accuracy. For this reason we have chosen it for the QM/MM calculations.
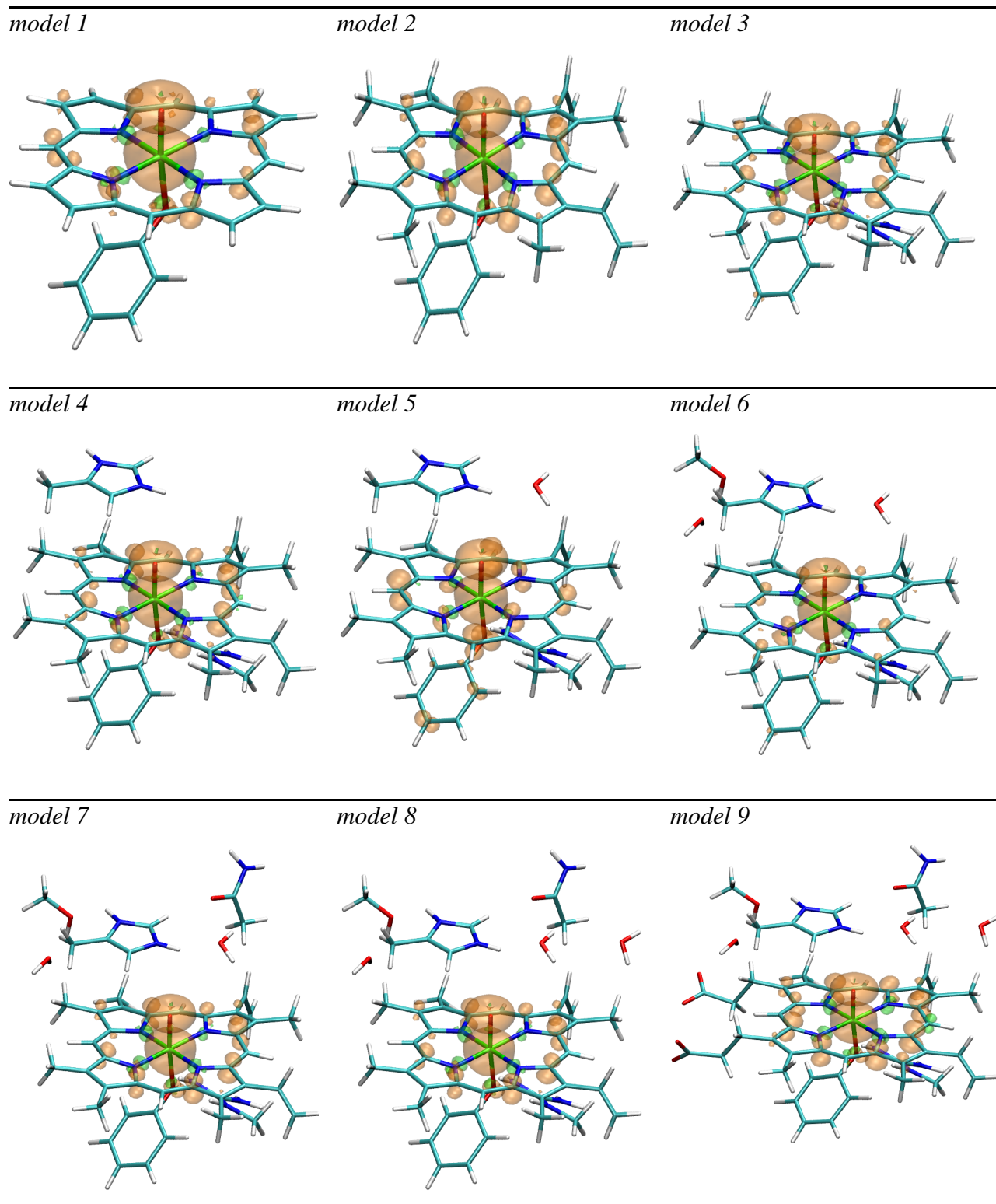
Figure S2. Models used to test the convergence of the electron affinity of the heme with respect to the size of the QM region. Only QM atoms are displayed. Spin isodensity surfaces (at 0.004 e Å^{-3}) corresponding to the oxidized state (i.e. Cpd I) are also shown.
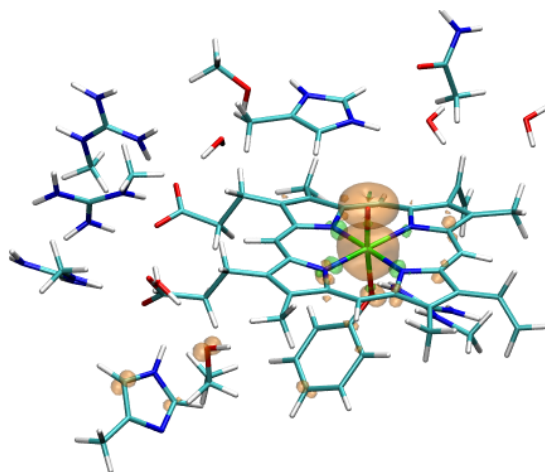
model 10

Figure S2 (*cont.*). Models used to test the convergence of the electron affinity of the heme with respect to the size of the QM region. Only QM atoms are displayed. Spin isodensity surfaces (at 0.004 e $Å^{-3}$) corresponding to the oxidized state (i.e. Cpd I) are also shown.

Table S1. Dependence of the electron affinity *ΔE* of HPC Cpd I on the number of QM atoms used in the QM/MM calculation.[a]

Model[b]	# QM atoms	ΔE^c	$\Delta E_{QM}{}^d$	$\Delta E_{QM\text{-}MM}{}^e$
1	50	-7.08	3.56	-10.64
2	76	4.35	3.44	0.91
3	89	4.63	5.49	-0.86
4	102	5.17	7.75	-2.58
5	105	5.17	7.77	-2.60
6	114	5.17	7.80	-2.63
7	123	4.90	7.64	-2.74
8	126	5.17	7.62	-2.45
9	136	4.63	3.84	0.79
10	202	4.90	8.73	-3.83

[a] All energies are in eV.
[b] See Figure S2 for an illustration of the QM models used.
[c] Eq. (14) in the main text.
[d] Contribution to ΔE due to QM subsystem.
[e] Contribution to ΔE due to QM-MM interactions.

2.2. Cutoff radius of the QM-MM electrostatic interactions

Table S2. Dependence of the electron affinity ΔE of HPC Cpd I on the cutoff radius of the QM-MM interactions. [a]

r_{NN} (Å)[b]	ΔE[c]	ΔE_{QM}[d]	$\Delta E_{QM\text{-}MM}$[e]
5.3	5.442	7.837	-2.395
10.6	5.442	7.836	-2.394
15.9	5.442	7.835	-2.396
21.2	5.442	7.835	-2.396
26.5	5.442	7.835	-2.396
529	5.442	7.839	-2.397
79.4	5.442	7.839	-2.397
105.8	5.442	7.839	-2.397
132.3	5.442	7.839	-2.397

[a] All energies are in eV.
[b] Cutoff radius of the QM-MM electrostatic interactions. For the MM atoms within a distance r_{NN} of any QM atom the electrostatic interaction energy between the QM and MM region was calculated by real space integration of the Coulomb interaction the full electron + nuclei density of the QM subsystem and the force field charges of the MM atoms. All other MM atoms beyond r_{NN} interact with the D-RESP charges assigned to the QM atoms.
[c] Eq. (14) in the main text.
[d] Contribution to ΔE due to the QM subsystem.
[e] Contribution to ΔE due to QM-MM interactions.

2.3. Sampling density

Table S3. Dependence of the ionization energy of HPC Cpd I on the sampling of gap energies.[a]

sampling density (ns)[b]	# configurations [c]	ΔE[d]	ΔE_{QM}[e]	$\Delta E_{QM\text{-}MM}$[f]
2	6	5.31 ± 0.38	7.81 ± 0.13	-2.50 ± 0.24
1	11	5.42 ± 0.33	7.86 ± 0.12	-2.44 ± 0.20
0.5	21	5.48 ± 0.30	7.89 ± 0.12	-2.41 ± 0.20

[a] All the energies are given in eV. The average $\pm$ the root mean square fluctuations are shown.
[b] Time interval between two classical MD snapshots taken for calculation of ΔE at the QM/MM level of theory
[c] [total simulation time (10 ns) / sampling density] + 1
[d] Eq. (14) in main text.
[e] Contribution to ΔE due to the QM subsystem.
[f] Contribution to ΔE due to QM-MM interactions.

3. QM/MM metadynamics simulations of proton transfer

3.1. Simulation details

Table S4. Parameters defining the collective variables CV_1 and CV_2 (d_{cut}, p and q, Eq. (16) in main text), and parameters defining the dynamics of the fictitious particle (mass M and force constant k) and the Gaussian history-dependent potential (height w and width δs) in QM/MM metadynamics calculations of proton transfer.

parameter	d_{cut} (Å)	P	Q	M (a.u)	k (a.u.)	w (kcal/mol)	δs
				HPC			
CV_1	0.8	6	15	30	6	1	0.02
CV_2	1.8	3	18	3	3	1	0.05
				PVC			
CV_1	1.0	3	9	1	6	0.5	0.07
CV_2	1.0	6	12	1	6	0.5	0.07

3. 2. Representative snapshots along the metadynamics trajectory
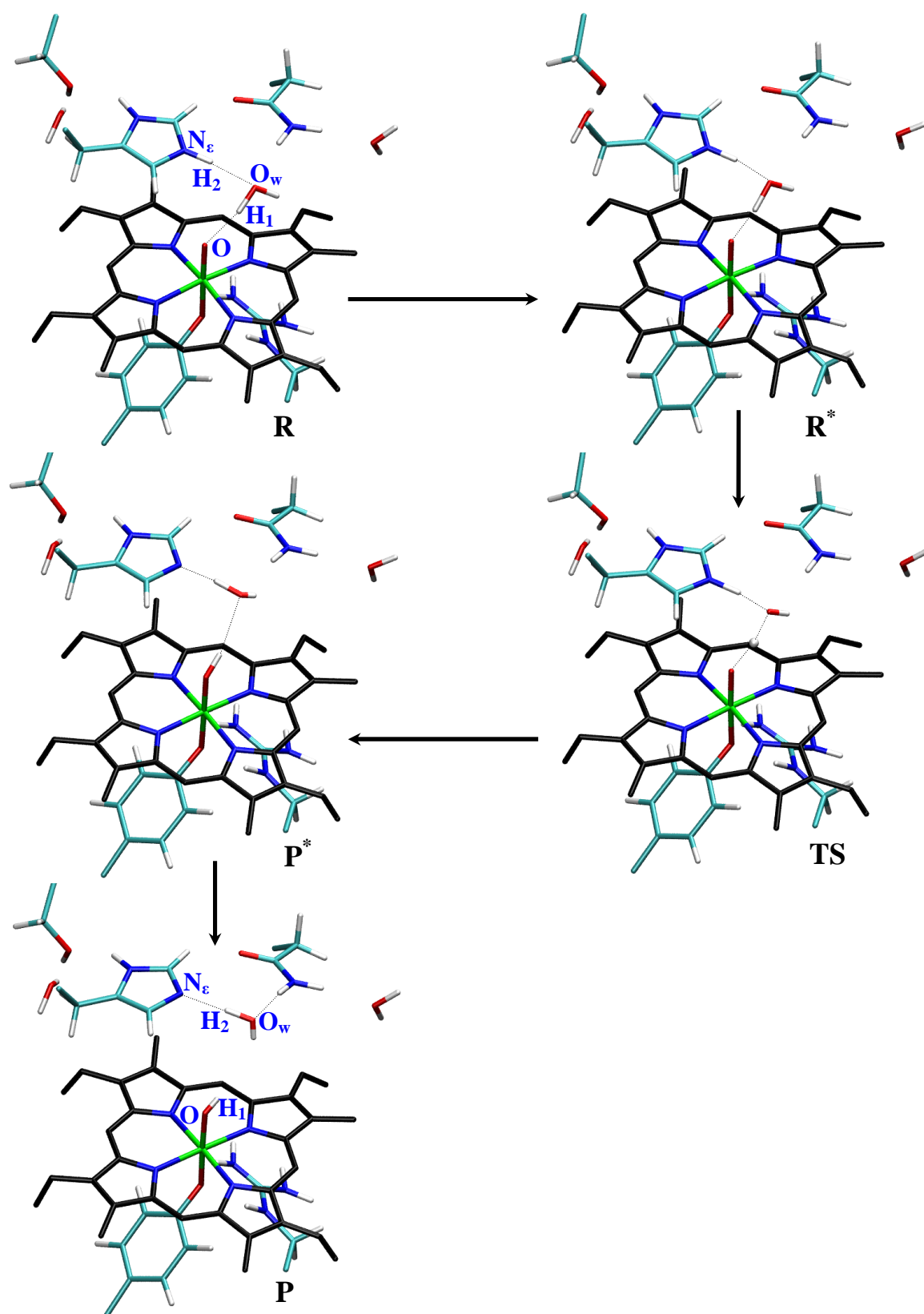

Figure S3. Atomic rearrangements along the PT pathway of HPC Cpd II. Average structures along the metadynamics simulation are shown. Only the QM atoms are displayed.
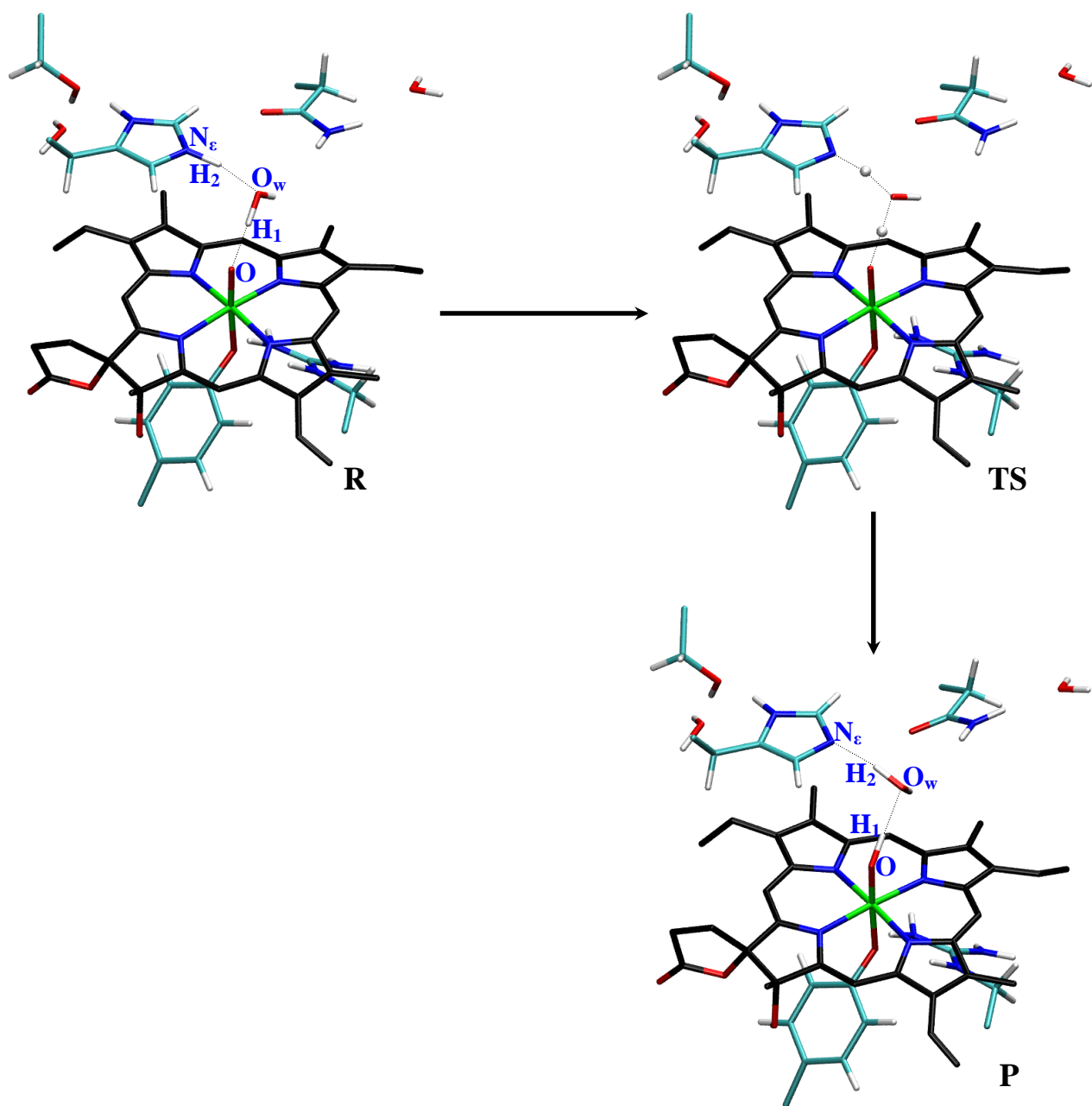
Figure S4. Atomic rearrangements along the PT pathway of PVC Cpd II. Average structures along the metadynamics simulation are shown. Only the QM atoms are displayed.

References

(1) de Visser, S. P. *Inorg. Chem.* 2006, 45, 9551-9557.

(2) Benecky, M. J.; Frew, J. E.; Scowen, N.; Jones, P.; Hoffman, B. M. *Biochemistry*. 1993, *32*, 11929-11933.

(3) Ivancich, A.; Jouve, H. M.; Sartor, B.; Gaillard, J. *Biochemistry*. 1997, *36*, 9356-9364.